



Radio-Wave Oscillations of Molecular-Chain Resonators

Stefan Müller,* Mohammad Rashidi, Karlheinz Mayr, Michael Fattinger, Andreas Ney, and Reinhold Koch
Institute of Semiconductor and Solid State Physics, Johannes Kepler University Linz, 4040 Linz, Austria
 (Received 20 December 2013; published 17 March 2014)

We report a new type of nanomechanical resonator system based on one-dimensional chains of only 4 to 7 weakly coupled small molecules. Experimental characterization of the truly nanoscopic resonators is achieved by means of a novel radio-frequency scanning tunneling microscopy detection technique at cryogenic temperatures. Above 20 K we observe concerted oscillations of the individual molecules in chains, reminiscent of the first and second eigenmodes of a one-dimensional harmonic resonator. Radio-frequency scanning tunneling microscopy based frequency measurement reveals a characteristic length dependence of the oscillation frequency (between 51 and 127 MHz) in reasonable agreement with one-dimensional oscillator models. Our study demonstrates a new strategy for investigating and controlling the resonance properties of nanomechanical oscillators.

DOI: 10.1103/PhysRevLett.112.117201

PACS numbers: 85.85.+j, 37.90.+j, 68.37.Ef, 84.40.-x

Resonant oscillators are ubiquitous in nature at all length scales. Meter-sized mechanical resonators have archetypal practical applications in musical instruments [1] and clocks [2]. At the microscopic length scale, mechanical resonators find their most prominent applications in scanning probe microscopy [3] as well as accurate detection of tiny masses [4,5] and forces [6–8]. While maintaining micrometer lengths, the reduction of the thickness of mechanical resonators down to the nanometer scale has even enabled insight into fundamentals of quantum mechanics [9–13]. Further reduction in all three spatial dimensions (width, thickness, and length) to the nanoscopic scale has so far remained elusive.

Here, we report an experimental study on a novel type of mechanical resonating “cantilever” consisting only of a few small molecules. It is based on one-dimensional chains of weakly interacting molecules adsorbed on a Au(111) surface. The fundamental characterization of the molecular-chain resonators is successfully demonstrated by means of a novel detection method utilizing a scanning tunneling microscope (STM) modified by a radio-frequency (rf) spectroscopic system (Fig. 1). Heating of the substrate above 20 K reveals concerted mechanical oscillations of the molecular chains, evidenced by the characteristic topographic “broadening” in the STM image (Fig. 2). Our rf STM detects characteristic frequencies of the molecular-chain resonators between 51 and 127 MHz with a chain-length dependence in reasonable agreement with a coupled-oscillator model.

The nanomechanical resonators investigated herein consist of the nonpolar stable π radical α, γ -bis(diphenylene- β -phenylallyl) (BDPA) [14] illustrated in Fig. 2(a). Recently, our group demonstrated the self-alignment of one-dimensional chains of BDPA molecules along the $\langle 11\bar{2} \rangle$ direction of the reconstructed Au(111) surface [15]. Chain formation, caused by weak unidirectional attraction

[15,16] between neighboring BDPA molecules, starts at triangular clusters of three molecules that act as nucleation centers [Figs. 2(b), (c)]. The experiments were performed with a commercial low-temperature STM (Createc) that we equipped with a dedicated rf circuitry with a bandwidth of 10 MHz to 1 GHz. Our setup is similar to that of Voigt *et al.* [17], who have shown that rf oscillations can be detected by STM even without the use of a dedicated impedance matching network employed by other groups [18–20]. Instead of using a frequency mixing technique with lock-in detection as in Refs. [17,21], here we couple out the rf component of the tunneling current via a bias T for direct detection of the rf current modulations with a spectrum analyzer. Figure 1 shows a schematics of our rf-STM experimental setup. The tunneling current signal is

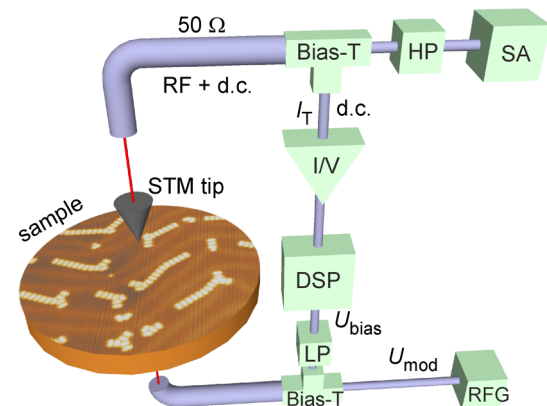


FIG. 1 (color online). Schematics of the rf-STM experimental setup, including I/V conversion and amplification (gain 10^8 , < 7 kHz), low-pass (LP) and high-pass (HP) filters, spectrum analyzer (SA), rf-signal generator (RFG), digital signal processing unit (DSP), and bias T s for separating dc and rf components of the tunneling current signal.

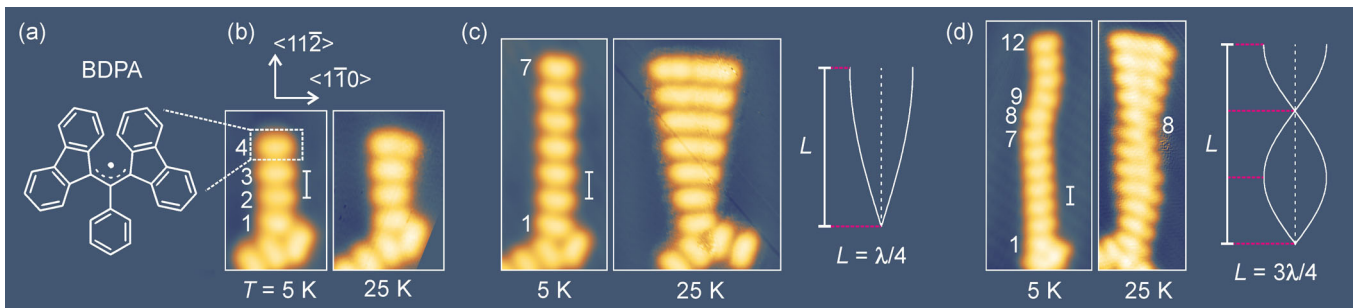


FIG. 2 (color online). One-dimensional resonators based on molecular chains of BDPA on Au(111). (a) Chemical structure of BDPA. (b)–(d) STM topographic images ($+1$ V, 50 pA) of BDPA chains obtained at a substrate temperature of 5 K (left) and 25 ± 5 K (right), scale bar = 0.73 nm, individual BDPA monomers are labeled by numbers 1–12. Insets: Illustration of first and second vibrational eigenmode of a one-dimensional harmonic resonator of length L and wavelength λ .

split into dc and rf components via a bias T . The dc component serves, as usual, as a feedback signal for maintaining a fixed tunneling current in the range of 40 to 100 pA at $+1$ V. The rf component is fed into a spectrum analyzer (Agilent MXA 9020) set to a bandwidth of 1 MHz. For obtaining the rf spectrum of a vibrating molecular chain, a recursive background subtraction procedure was applied based on averaging consecutive difference spectra between the oscillating molecular chain and the background signal of the pristine Au(111) surface. Impurity and tip effects during STM measurement were minimized by multiple tip formings between the experiments, resulting in Au-coated tips. Reliable tip performance was established by accurately reproducing the characteristic conductance signature of the Au(111) surface state well known from the literature [22]. Possible tip effects on the chain oscillations were minimized by positioning the STM tip close to the rim of the oscillating chains.

Observation of nanochain vibration.—For the present work we studied more than 100 different BDPA chains with a length of 3 to 12 monomers at “soft” tunneling conditions ($+1$ V, 50 pA). Figure 2(b) (left) shows a typical STM image of a chain of four BDPA monomers denoted in the following as “4-chain.” The image was obtained at a substrate temperature of 5 K, where lateral motion of BDPA on Au(111) is effectively “frozen out” and, therefore, all individual monomers in a chain have the same topographic appearance. The monomers are imaged as “bean-shaped” protrusions separated by 0.73 nm along the chain direction. The individual monomers of the 4-chain in Fig. 2(b) are labeled by numbers 1 to 4 . The first monomer (1) of the chain is part of the triangular cluster (visible in the bottom part of the image) and therefore pinned. The last monomer (4), on the other hand, is not pinned, thus, representing the “free end” of the chain. Figures 2(c), (d) (left) show representative examples of a 7-chain and a 12-chain, consisting of 7 and 12 monomers, respectively.

Increasing the substrate temperature to 25 K causes a dramatic change of the STM topographic appearance of the

BDPA chains. The chains are significantly broadened in the $\langle 1\bar{1}0 \rangle$ direction perpendicular to the chain axis, as exemplified in Figs. 2(b), (c) (right) for 4- and 7-chains. Transverse broadening is clearly discernible by comparing the right and left images of Figs. 2(b), (c) obtained at 25 and 5 K, respectively. The monomer separation along the chain axis is the same at both temperatures. The magnitude of the transverse broadening is maximal at the free end of the chain and decays monotonically towards the fixed end. Consequently, we denote the fixed end as “node” and the free end as “antinode.” The characteristic broadening observed at 25 K indicates transverse mechanical vibrations of the individual monomers in the chain relative to the Au(111) surface. The individual monomers are imaged in a homogeneously blurred manner, suggesting that the vibration occurs on a time scale much faster than both the scan speed of the STM tip (1 sec per scanned line) as well as the bandwidth of the STM feedback loop (few kHz). Obviously, the monomers undergo several cycles of transverse vibration while the STM tip scans the image of the whole chain. The total broadening of the individual monomers in chains represent their maximum deflection amplitudes during several cycles of vibration.

In the case of chains longer than 7 monomers, we frequently observe one or more additional nodes (equal to monomers with minimum transverse motion) located between the free and fixed ends. Figure 2(d) (right) shows a vibrating 12-chain at 25 K with an additional node at monomer position 8 . The extra node lies at approximately $2/3$ of the total chain length from the fixed end (monomer 1) of the 12-chain. This property is stunningly similar to the nodal structure of the second eigenmode of a one-dimensional harmonic resonator of length L and wavelength λ illustrated in the inset of Fig. 2(d). In fact, a detailed analysis of the vibrating BDPA chains studied in the present work confirms that the separation of nodes and adjacent antinodes amounts to approximately $\lambda/4$, which is consistent with the eigenmodes of a one-dimensional harmonic resonator [compare insets of Figs. 2(c), (d)]. The observed structures of nodes and antinodes in proper

separation along the chains provide conclusive evidence that the molecular chains undergo (periodic) oscillatory motion at a particular frequency f . Random motion, on the contrary, is unable to explain the observed $\lambda/4$ periodicity of the topographic broadening. The node or antinode pattern suggests that the individual monomers of the chains oscillate in a concerted manner—consistent with intermolecular coupling within chains [15].

In contrast to the oscillating BDPA chains, no broadening is observed for the Au herringbone pattern. This evidences that the phonon amplitudes of the Au(111) atomic lattice are very small (below the spatial resolution of STM) compared to the observed chain deflection amplitudes. Furthermore, it indicates that the chains oscillate independent of the substrate atomic lattice—consistent with the weak physisorption of BDPA on Au(111) as well as the huge difference in frequencies of the phonons and the BDPA chains (see below).

What drives the chain vibration: Role of the thermal bath.—Our STM investigations evidence that chain vibration abruptly sets in close to a substrate temperature of 20 K. At lower temperatures (≤ 15 K) the BDPA chains appear static in STM images, suggesting that they are in the vibrational ground state. The observed temperature-induced onset of chain vibration indicates that thermal excitation by the “heat bath” of the substrate surface is responsible for the motion of the BDPA chains. Since we observe rather specific (transverse) modes of chain oscillation, the thermal activation argument requires a more detailed discussion of the available phonons with energies close to $k_B T$ (Boltzmann constant k_B).

The onset behavior can be explained by the phonon dispersion of the reconstructed Au(111) surface shown in Fig. 3(a) (extracted from Ref. [23]). The surface phonons of Au(111) are indicated as circles (experimental) and lines (calculated), respectively, and bulk phonons as shaded regions. Because of the Boltzmann occupation, at 5 K predominantly those phonons are excited that have wave vectors k close to the $\bar{\Gamma}$ point of the surface Brillouin zone. The respective phonon wavelength $\lambda = 2\pi/k$ is very large, i.e., similar to or exceeding the length of the BDPA chains. We deduce from Fig. 3(a) for a phonon energy equal to $E/k_B = 5$ K a maximum wave vector of $k = 0.05 \text{ \AA}^{-1}$ in the $\bar{\Gamma}\bar{M}$ direction (i.e. transverse to the chain axis). This corresponds to a phonon wavelength as large as 13 nm. Phonons with such long wavelengths are expected to “offset” the chain as a whole rather than to excite its vibration. In order to excite transverse chain vibration, however, the phonon wavelength is expected to be of the order of $\lambda/4 = r$ as illustrated in Fig. 3(b), where r is the monomer separation along the chain. This condition assures that the individual monomers of a chain may receive transverse kicks by the phonons that can excite the vibration of the whole chain. From the experimental value of $r = 0.73 \text{ nm}$ along the BDPA chain [15], a phonon

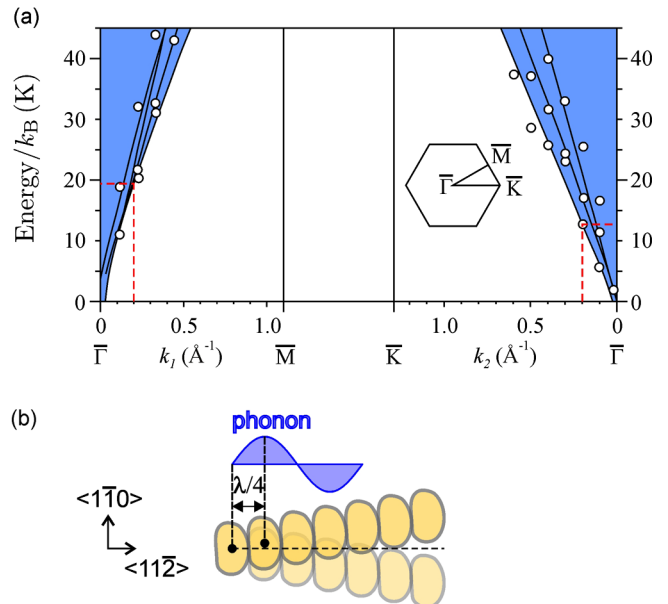


FIG. 3 (color online). (a) Phonon dispersion of the reconstructed Au(111), solid lines: calculated dispersion curves of surface phonons extracted from Ref. [23], circles: experimental data from Ref. [24], shaded regions: energies of bulk phonons projected on the surface high-symmetry lines. (b) Illustration of a substrate phonon with wavelength λ exciting individual monomers of a chain by transverse “kicks.”

wave vector of $k = 2\pi/4r = 0.22 \text{ \AA}^{-1}$ is estimated. According to Fig. 3(a), transverse phonons along $\bar{\Gamma}\bar{M}$ with a similar wave vector, suitable for exciting chain vibration, have energies equivalent of $E/k_B = 20 \text{ K}$ and more (indicated by the dashed line). Only at a substrate temperature of 20 K and above does a reasonable fraction of respective phonons become thermally populated (e.g., $\approx 37\%$ for $E_{\text{phonon}} = k_B T$). This is in good agreement with the onset of BDPA chain vibration observed in this study.

Observation of characteristic radio-frequency signal on vibrating chains.—While the amplitude of a single vibrating chain may be directly deduced from the transverse broadening in the STM image (see Fig. 2), experimental determination of the vibration frequency (f) of the chain by STM is not straightforward. Since the above results indicate a value of f much larger than the bandwidth of the STM current amplifier of 50 kHz, conventional STM electronics is unable to detect it.

To obtain a reasonable estimate of the frequency range expected for the oscillating BDPA chains, we take as a starting point Young’s modulus of weakly interacting hydrocarbon molecular thin films, with typical values ranging from $Y = 30 \text{ MPa}$ to 2 GPa [25]. The present case of reduced dimensionality (one-dimensional chains) compared to molecular thin films suggests to replace Young’s modulus by the (lower) shear modulus $G = Y/(2 + 2\nu) \approx 0.38Y$, using a typical Poisson ratio of $\nu = 0.33$. Furthermore, a film thickness below 1 nm

is expected to further reduce the elastic constants [26] by 70%. Assuming a rodlike cantilever with one fixed end, we calculate a vibration frequency of 150 MHz to 1.2 GHz, using the cantilever formula [10]

$$f = \frac{1}{4\pi} \frac{t}{L^2} \sqrt{\frac{G}{\rho}} \quad (1)$$

based on continuum mechanics. We have used spatial dimensions similar to the BDPA chains; i.e., thickness $t = 0.7$ nm, length $L = 4.38$ nm (equivalent to a 7-chain), bulk density $\rho = 1300$ kg/m³, and elastic constant G reduced to 3.4–230 MPa as discussed above. Our rf STM is equipped with an additional rf wiring and detection system [17] in order to detect rf current signals with a bandwidth ranging from 10 MHz to 1 GHz (Fig. 1). Thus, the experimental bandwidth is expected to suffice the detection of the vibration frequency of the BDPA chains.

It is important to exclude effects of pinning of BDPA monomers to specific surface sites that may predefine certain monomers as nodes of the vibrating chain. Therefore, we focus, in the following, exclusively on vibrating BDPA chains that exhibit only one node defined by the triangular BDPA structure at one end of the chain similar to those shown in Figs. 2(b), (c).

Since the chain vibration is much faster than the feedback of the STM (see above), the tip height is unaffected by the chain vibration. Positioning the STM tip close to the rim of a vibrating chain at the soft tunneling condition enables the chain to periodically move in and out of the tunnel junction, thus modulating the tunneling distance and, consequently, the tunneling current at the frequency of the chain vibration. Our experiments show that when the STM tip is positioned close to the rim of a vibrating chain, indeed, a distinct peak can be observed in the rf spectrum of the tunneling current. A similar result is obtained by scanning a small area including the rim of the free end of vibrating chains. Figure 4(a) shows exemplarily the rf spectrum of the tunneling current obtained for a 5-chain (circles). The main contribution to the spectrum is an almost symmetric peak at 98 MHz with a signal-to-noise ratio of about 3 dB. The spectral width of 2.5 MHz indicates a quality factor of $Q \approx 40$. No other significant f_c signals were observed between 10 and 1 GHz (not shown). We denote the peak position as the “characteristic frequency” (f_c). When placing the tip over static (pinned) BDPA or over the bare Au(111) substrate, no f_c signal is observed, evidencing the direct relation of the f_c signal to the chain vibration.

We want to emphasize that measuring the f_c of BDPA chains is indeed an experimental challenge, both with respect to the sample and with respect to the measuring process. The f_c signal is detectable only for oscillating

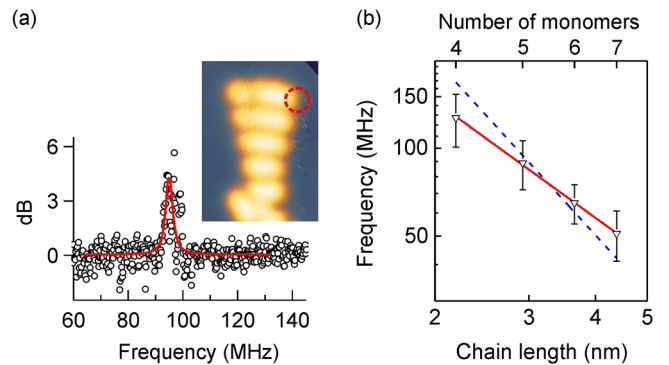


FIG. 4 (color online). Measurement of rf signals from vibrating molecular chains of BDPA on Au(111). (a) rf spectrum of the tunneling current obtained from an oscillating 5-chain at 24 K, STM tip operated at 40 pA and +1 V over the position marked by a circle in the inset, solid line is a guide to the eye, 0 dB refers to the noise floor of the rf detection system of 37 pA/ $\sqrt{\text{Hz}}$. Inset: STM image of vibrating 5-chain. (b) Double-logarithmic plot of the characteristic frequency vs. the chain length for vibrating BDPA chains with 4 to 7 monomers, solid line: numerical fit with function $\propto 1/L^{1.3}$, dashed line: numerical fit with function $\propto 1/L^2$.

chains, but it turns out that not all of the vibrating chains are suitable for obtaining the f_c signal. In particular, longer chains may be locally pinned at defects of the substrate and therefore may not vibrate uniformly. Minimization of possible interactions of the STM tip with the weakly physisorbed molecular chains by careful optimization of the tunneling parameters turned out to be essential for a successful measurement of the f_c by STM. Overdamping effects by the STM tip were found to increase with the chain length; no reliable f_c values could be obtained for chains longer than 7-chains. Based on our experiments, we estimate the success rate for observing a f_c signal from vibrating chains with a signal-to-noise ratio ≥ 3 dB to about < 5% for our best tips.

Figure 4(b) shows the compiled results of successful measurements of the f_c signal on vibrating BDPA chains with lengths between 4 and 7 monomers obtained at 25 K. We were able to obtain 2–4 independent f_c values for each chain length shown in Fig. 4(b), with the error bars reflecting the experimental deviations of the individual frequency measurements. With an increasing chain length, we observe a decrease of the f_c value from 127 ± 26 MHz (4-chains) down to 51 ± 10 MHz (7-chains). The length dependence is well approximated by a $1/L^b$ function with an exponent of $b = 1.3$ obtained by a least-squares fit as indicated by the solid line (red) in Fig. 4(b). In contrast, the model of Eq. (1), based on continuum mechanics, predicts a value of $b = 2$ (dashed blue curve). Obviously, the observed behavior of BDPA chains lies between the two limiting cases of continuum mechanics and a discrete coupled-oscillator model with $b = 1$.

Conclusions.—In conclusion, the BDPA chains as a whole can be regarded as mechanical nanoresonators. Their spatial dimensions are at least 1 order of magnitude smaller than the smallest free-standing nanoelectromechanical resonators reported in the literature [27,28] and their mass is several orders of magnitude smaller (monomer mass is $m_0 = 6.95 \times 10^{-25}$ kg). The experimental results obtained with our novel rf-STM technique evidence that the characteristic frequency values (f_c) obtained on vibrating BDPA chains reflect their oscillation frequencies—in reasonable agreement with common dynamical models.

We thank Ch. Diskus and R. Rudersdorfer for helpful input on setting up our rf circuitry as well as W. Jantsch for fruitful discussions. We kindly acknowledge financial support of the projects P20773 and I958 by the Austrian Science Fund (FWF).

*stefan.muellegger@jku.at

- [1] N. H. Fletcher, *Rep. Prog. Phys.* **62**, 723 (1999).
- [2] A. M. Lepschy, G. A. Mian, and U. Viaro, *IEEE Trans. Ed.* **35**, 3 (1992).
- [3] G. Binnig, C. F. Quate, and C. Gerber, *Phys. Rev. Lett.* **56**, 930 (1986).
- [4] A. Gupta, D. Akin, and R. Bashir, *Appl. Phys. Lett.* **84**, 1976 (2004).
- [5] Y. T. Yang, C. Callegari, X. L. Feng, K. L. Ekinci, and M. L. Roukes, *Nano Lett.* **6**, 583 (2006).
- [6] J. J. Saenz, N. Garcia, P. Grütter, E. Meyer, H. Heinzelmann, R. Wiesendanger, L. Rosenthaler, H. R. Hidber, and H. J. Güntherodt, *J. Appl. Phys.* **62**, 4293 (1987).
- [7] M. F. Bocko and R. Onofrio, *Rev. Mod. Phys.* **68**, 755 (1996).
- [8] D. Rugar, R. Budakian, H. J. Mamin, and B. W. Chui, *Nature (London)* **430**, 329 (2004).
- [9] V. B. Braginsky and F. Y. Khalili, *Quantum Measurement*, edited by K. S. Thorne (Cambridge University Press, Cambridge, 1992).
- [10] M. Blencowe, *Phys. Rep.* **395**, 159 (2004).
- [11] K. R. Brown, C. Ospelkaus, Y. Colombe, A. C. Wilson, D. Leibfried, and D. J. Wineland, *Nature (London)* **471**, 196 (2011).
- [12] J. Chan, T. P. Mayer Alegre, A. H. Safavi-Naeini, J. T. Hill, A. Krause, S. Gröblacher, M. Aspelmeyer, and O. Painter, *Nature (London)* **478**, 89 (2011).
- [13] M. Poot and H. S. J. van der Zant, *Phys. Rep.* **511**, 273 (2012).
- [14] C. F. Koelsch, *J. Am. Chem. Soc.* **79**, 4439 (1957).
- [15] S. Müllegger, M. Rashidi, M. Fattinger, and R. Koch, *J. Phys. Chem. C* **116**, 22587 (2012).
- [16] S. Müllegger, M. Rashidi, M. Fattinger, and R. Koch, *J. Phys. Chem. C* **117**, 5718 (2013).
- [17] P. U. Voigt and R. Koch, *J. Appl. Phys.* **92**, 7160 (2002).
- [18] Y. Manassen, R. J. Hamers, J. E. Demuth, and A. J. Castellano, Jr., *Phys. Rev. Lett.* **62**, 2531 (1989).
- [19] R. J. Schoelkopf, P. Wahlgren, A. A. Kozhevnikov, P. Delsing, and D. E. Prober, *Science* **280**, 1238 (1998).
- [20] U. Kemiktarak, T. Ndakum, K. C. Schwab, and K. L. Ekinci, *Nature (London)* **450**, 85 (2007).
- [21] V. Sazonova, Y. Yaish, H. Üstünel, D. Roundy, T. A. Arias, and P. L. McEuen, *Nature (London)* **431**, 284 (2004).
- [22] C. J. Chen, *Introduction to Scanning Tunneling Microscopy* (Oxford University Press, New York, 2008), 2nd ed.
- [23] X. Q. Wang, *Phys. Rev. Lett.* **67**, 1294 (1991).
- [24] U. Harten, J. P. Toennies, and C. Wöll, *Faraday Discuss. Chem. Soc.* **80**, 137 (1985).
- [25] S.-W. Hahm, H.-S. Hwang, D. Kim, and D.-Y. Khang, *Electron. Mater. Lett.* **5**, 157 (2009).
- [26] P. Villain, P. Beauchamp, K. F. Badawi, P. Goudeau, and P. O. Renault, *Scr. Mater.* **50**, 1247 (2004).
- [27] H. G. Craighead, *Science* **290**, 1532 (2000).
- [28] K. C. Schwab and M. L. Roukes, *Phys. Today* **58**, 36 (2005).